Electromagnetic electron-positron pair production in heavy-ion collisions with impact parameter zero

Kai Hencken and Dirk Trautmann
Institut für Theoretische Physik der Universität Basel, Klingelbergstrasse 82, 4056 Basel, Switzerland

Gerhard Baur
Institut für Kernphysik (Theorie), Forschungszentrum Jülich, 52425 Jülich, Germany
(Received 30 August 1993; revised manuscript received 20 October 1993)

We present a calculation of the second-order process of electron-positron pair creation by the electromagnetic fields of two relativistic heavy ions for impact parameter b zero. Total probabilities as well as differential ones are presented. A comparison with the results of the double equivalent-photon approximation (DEPA) shows explicitly the inapplicability of this approximation in the case of total probabilities. We discuss the creation of pairs with large invariant mass. The DEPA results are too high, which can be traced back to the mass singularity of the photon cross section at very small angles, giving a discrepancy, whereas the agreement between our result and DEPA is good for larger angles.
PACS number(s): 12.20.−m, 34.10.+x, 14.60.Cd

I. INTRODUCTION

We investigate the electromagnetic production of electron-positron pairs in the collision of two relativistic heavy ions. The interest in this is mainly based on the fact that the impact-parameter-dependent total probability of the pair creation in lowest order exceeds one for realistic accelerator parameters, so that higher-order effects—especially the multiple pair production—may be of importance [1–3]. These probabilities were mainly calculated using the so-called "equivalent-photon approximation" (EPA) also known as the Weizsäcker-Williams method [4,5]. This approximation is only justified for impact parameter b larger than the Compton wavelength of the electron. As the probability increases with smaller b, better calculations in this area are needed. Therefore the double equivalent-photon approximation (DEPA) was proposed to do the calculations. But the DEPA needs a cutoff parameter, too, whose value is not given *a priori*. An exact treatment of the pair production should give some insight into the applicability of the DEPA. For a review of the existing calculations see [6].

In Sec. II we derive the matrix element for the pair production by an external field in second order. We use the field of two colliding heavy ions with impact parameter b—with and without form factor—and then specialize to the case $b=0$. In Sec. III this matrix element is further reduced and the Feynman integrals occurring in it are solved analytically. This gives us the differential probability $P(p_+,p_-)$. In Sec. IV, we derive the corresponding result for the DEPA. In Sec. V, we discuss the total probability P_{total}. Results for some realistic heavy-ion accelerators are presented. We compare the total probability of our calculation with the DEPA. We find that the DEPA result exceeds our result, as soon as the parameter Λ controlling the width of the form factor becomes larger than the electron mass. In Sec. VI, we show results of our calculation for a number of single-differential probabilities.

It has been argued that DEPA should again be usable for pairs with large invariant mass. In Sec. VII, we discuss this special case, finding that there is a discrepancy between our results and DEPA. The reason for this is the mass singularity of the photon cross section at very small angles, whereas for larger angles we find good agreement with DEPA.

In the future, more calculations will be done, in order to study systematically the dependence of the probability on the different parameters (m_e,Λ,γ,b) in different sections of the phase space.

In the Appendices we summarize how to calculate the Feynman integrals occurring in our calculation and discuss the two form factors for the heavy ions we use in our calculations.

Throughout this paper, we use the following convention: the metric is $(1,-1,-1,-1)$, and the Dirac spinors are normalized as

$$\bar{u}_r(p)u_s(p)=2m\delta_{rs},\quad \bar{v}_r(p)v_s(p)=-2m\delta_{rs}\ . \tag{1}$$

The four-dimensional Fourier transformation is chosen as

$$f(x^\mu)=\int\frac{d^4p}{(2\pi)^4}\hat{f}(p^\mu)\exp(-ip^\nu x_\nu)\ , \tag{2a}$$

$$\hat{f}(p^\mu)=\int d^4x f(x^\mu)\exp(ip^\nu x_\nu)\ , \tag{2b}$$

to be consistent with the decomposition into free solutions. Since we write the wave equation of the electromagnetic potential as

$$\Box A^\mu(x)=j^\mu(x) \tag{3}$$

the fine-structure constant has to be defined as $\alpha:=e^2/(4\pi)$.

II. THE MATRIX ELEMENT IN SECOND ORDER

We describe the interaction with the heavy ions as an interaction with the external field produced by both ions. We restrict ourself to lowest order, which for this process is the second. This has been studied for the first time by Landau and Lifshitz [7], see also [8,9]. The process is shown in Fig. 1. Its matrix element is

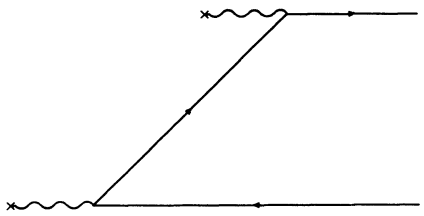

FIG. 1. General form of the second-order diagram for pair creation in an external field.

$$M=-ie^2\bar{u}(p_-)\times\int\frac{d^4p}{(2\pi)^4}A(p_--p)\frac{\not p+m}{p^2-m^2}A(p_++p)v(p_+)=:\bar{u}(p_-)\hat{M}v(p_+)\ . \tag{4}$$

Here we have introduced the matrix element without Dirac spinors $\hat{M}$. From this the unpolarized differential probability to produce an electron with momentum p_- and a positron with p_+ is given by

$$P=\sum_{s_+s_-}|M|^2\frac{d^3p_+d^3p_-}{4\epsilon_+\epsilon_-(2\pi)^6}=\mathrm{Tr}((\not p_-+m)\hat{M}(\not p_+-m)\bar{\hat{M}})\frac{d^3p_+d^3p_-}{4\epsilon_+\epsilon_-(2\pi)^6}\ , \tag{5}$$

using the standard method to rewrite the polarization summation as a trace.

The external electromagnetic field is produced by the two heavy ions, i.e., we neglect the effect of the process on the ions itself, as well as the Coulomb repulsion of the ions on each other. The heavy ions are then moving on a straight line. The potential of a point charge Q, moving along a straight line with four-velocity u^μ and at distance r from the origin, is

$$A^\mu(q)=-2\pi Qu^\mu\frac{1}{q^2}\delta(qu)\exp(iqr)\ . \tag{6}$$

As we will see later, the total probability to produce a pair diverges, if we use a point charge. We therefore introduce a form factor to describe the extended charge distribution of the heavy ion:

$$A^\mu(q)=-2\pi Qu^\mu\frac{F(q^2)}{q^2}\delta(qu)\exp(iqr)\ . \tag{7}$$

The form factors used throughout the calculations are the dipole form factor

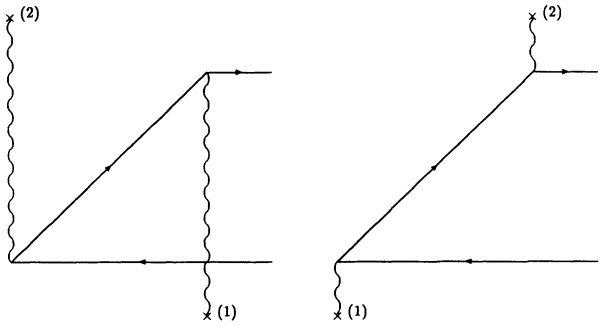

FIG. 2. The two diagrams contributing to the pair creation in the heavy-ion collisions, where (1) and (2) denote the interaction with the field of ions 1 and 2, respectively.

$$F_{\mathrm{dipole}}(q^2)=\frac{\Lambda^2}{\Lambda^2-q^2} \tag{8}$$

and a form factor, which is the sum of two dipole form factors

$$F_{\mathrm{double}}(q^2)=c_1\frac{\Lambda_1^2}{\Lambda_1^2-q^2}+c_2\frac{\Lambda_2^2}{\Lambda_2^2-q^2}\ , \tag{9}$$

called by us the "double dipole form factor."

In Appendix B we show how to choose the parameters in the form factors. The dipole form factor is that of a Yukawa charge distribution, which is surely not very realistic. On the other hand, the probabilities are normally not very sensitive to the detailed form of the form factor, and we can treat $\hat{M}$ analytically using (8) and (9).

The field produced by both ions is then

$$A_\mu(q)=-2\pi e\frac{F(q^2)}{q^2}[Z_1u_\mu^{(1)}\delta(qu^{(1)})\exp(iqb/2)+Z_2u_\mu^{(2)}\delta(qu^{(2)})\exp(-iqb/2)]\ . \tag{10}$$

In the following, we consider only symmetric configurations, where both ions are identical: $Z=Z_1=Z_2$ and choose the c.m. system, so that $\gamma=\gamma_1=\gamma_2$. This corresponds to $\gamma_L=2\gamma^2-1$ for one ion in the laboratory system of a fixed target machine. We will neglect at the moment the form factor $F(q^2)$, as its inclusion in the formulas is straightforward, but come back to it at the end.

With this potential, there are four possible combinations in $\hat{M}$, but only two of them are allowed kinematically (see Fig. 2). Therefore we have

$$\begin{aligned}\hat{M}&=-ie^2\left[\int\frac{d^4p}{(2\pi)^4}\not A^{(1)}(p_--p)\frac{\not p+m}{p^2-m^2}\not A^{(2)}(p_++p)+\int\frac{d^4p}{(2\pi)^4}\not A^{(2)}(p_--p)\frac{\not p+m}{p^2-m^2}\not A^{(1)}(p_++p)\right]\\&=-i\left[\frac{Ze^2}{2\pi}\right]^2\left[\not u^{(1)}\int d^4p\frac{\not p+m}{(p_--p)^2(p^2-m^2)(p_++p)^2}\not u^{(2)}\delta((p_--p)u^{(1)})\delta((p_++p)u^{(2)})\right.\\&\quad\times\exp(-ipb)\exp[i(p_--p_+)b/2]\\&\quad\left.+\not u^{(2)}\int d^4p\frac{\not p+m}{(p_--p)^2(p^2-m^2)(p_++p)^2}\not u^{(1)}\delta((p_--p)u^{(2)})\delta((p_++p)u^{(1)})\right.\\&\quad\left.\times\exp(+ipb)\exp[-i(p_--p_+)b/2]\right]\ .\end{aligned} \tag{11}$$

We now restrict ourself to the case where the impact parameter b is zero. In $\hat{M}$, b only occurs in the exponent, multiplied by some transverse momenta $p_\perp$. As we will see later in the discussion of P_{total}, mainly small $p_\perp$ contributes to the total probability, smaller than Λ (of the form factor) and also mainly smaller than m_e. The case $b=0$ can therefore be seen as the first term of an expansion in $p_\perp b$, which should surely be good, as long as b is smaller than the nuclear radius and should not be to different for b smaller than the Compton wavelength: $b < \lambda\!\!\!^{-}_C = 1/m_e$. $\hat{M}$ for $b=0$ is then

$$\hat{M} = -i\left[\frac{Ze^2}{2\pi}\right]^2 \left[\not{u}^{(1)} \int d^4p \frac{\not{p}+m}{(p_- - p)^2(p^2-m^2)(p_+ + p)^2} \not{u}^{(2)} \delta((p_- - p)u^{(1)})\delta((p_+ + p)u^{(2)}) \right.$$
$$\left. + \not{u}^{(2)} \int d^4p \frac{\not{p}+m}{(p_- - p)^2(p^2-m^2)(p_+ + p)^2} \not{u}^{(1)} \delta((p_- - p)u^{(2)})\delta((p_+ + p)u^{(1)}) \right] . \tag{12}$$

III. EXACT SOLUTION OF THE MATRIX ELEMENT

In order to find an analytical form for the matrix element, we have to integrate over the internal momentum. First we define

$$I_D^{(m,i)} := \int d^4p \frac{\{m, p_i\}}{(p_- - p)^2(p^2-m^2)(p_+ + p)^2} \times \delta((p_- - p)u^{(1)})\delta((p_+ + p)u^{(2)}) , \tag{13a}$$

$$I_X^{(m,i)} := \int d^4p \frac{\{m, p_i\}}{(p_- - p)^2(p^2-m^2)(p_+ + p)^2} \times \delta((p_- - p)u^{(2)})\delta((p_+ + p)u^{(1)}) , \tag{13b}$$

which are the integrals occurring in the "direct" and "exchanged" diagram, giving for $\hat{M}$

$$\hat{M} = -i\left[\frac{Ze^2}{2\pi}\right]^2 [\not{u}^{(1)}(I_D^{(i)} + I_D^{(m)})\not{u}^{(2)} + \not{u}^{(2)}(I_X^{(i)} + I_X^{(m)})\not{u}^{(1)}] . \tag{14}$$

Now we use the two δ functions to reduce the four-dimensional integration. The four-velocities $u^{(1)}$ and $u^{(2)}$ in the c.m. frame are

$$u^{(1)} = \gamma(1,0,0,\beta) =: \gamma w^{(1)} , \tag{15a}$$

$$u^{(2)} = \gamma(1,0,0,-\beta) =: \gamma w^{(2)} . \tag{15b}$$

Evaluating them determines the zero and z component of the internal momentum. For the "direct" diagram, they are

$$\epsilon = \epsilon_D := \tfrac{1}{2}(\epsilon_- - \epsilon_+) - \tfrac{1}{2}\beta(p_{-z} + p_{+z}) , \tag{16a}$$

$$p_z = p_D := \tfrac{1}{2}(p_{-z} - p_{+z}) - \frac{1}{2\beta}(\epsilon_- + \epsilon_+) , \tag{16b}$$

and for the "exchanged" diagram

$$\epsilon = \epsilon_X := \tfrac{1}{2}(\epsilon_- - \epsilon_+) + \tfrac{1}{2}\beta(p_{-z} + p_{+z}) , \tag{17a}$$

$$p_z = p_X := \tfrac{1}{2}(p_{-z} - p_{+z}) + \frac{1}{2\beta}(\epsilon_- + \epsilon_+) . \tag{17b}$$

The only difference between both formulas is the sign between the two terms, which comes from the exchange of $\beta \leftrightarrow -\beta$ in the four-velocities.

We now split p into its longitudinal and transverse part defining

$$p_{Dl} := (\epsilon_D, 0, 0, p_D), \quad p_{Xl} := (\epsilon_X, 0, 0, p_X) , \tag{18}$$

and the same with p_- and p_+. The integral $I_D^{(m,i)}$ is now

$$I_D^{(m,i)} = \frac{1}{2\gamma^2\beta} \int d^2p_\perp \frac{\{m, p_i\}}{[(p_{-l} - p_{Dl})^2 + (p_{-\perp} - p_\perp)^2][p_{Dl}^2 + p_\perp^2 - m^2][(p_{+l} + p_{Dl})^2 + (p_{+\perp} + p_\perp)^2]} \tag{19}$$

and similar for $I_X^{(m,i)}$, changing p_{Dl} to p_{Xl}. Note that $p_\perp$ only has spatial components; evaluating the scalar products gives then an extra minus sign. The factor $1/2\gamma^2\beta$ comes from the evaluation of the δ functions.

Examining I_D and I_X for m, 0, and z, we find that the numerator of the integrand does not depend on $p_\perp$ and therefore we can rewrite them as

$$I_D^{(m,0,z)} = \frac{1}{2\gamma^2\beta}\{m, \epsilon_D, p_D\} \int d^2p_\perp \frac{1}{[(p_{-l} - p_{Dl})^2 + (p_{-\perp} - p_\perp)^2][p_{Dl}^2 + p_\perp^2 - m^2][(p_{+l} + p_{Dl})^2 + (p_{+\perp} + p_\perp)^2]} \tag{20}$$

and the corresponding result for $I_X^{(m,0,z)}$. As we show in Appendix A, the integral on the right side is just one of the standard integrals, the scalar three-term integral. Therefore we can write

$$I_D^{(m,0,z)} = -\frac{1}{2\gamma^2\beta}\{m, \epsilon_D, p_D\} I^S(k_{2D}, k_{3D}, m_{1D}^2, m_{2D}^2, m_{3D}^2)$$
$$=: -\frac{1}{2\gamma^2\beta}\{m, \epsilon_D, p_D\} I_D^S \tag{21}$$

with

$$k_{2D}=-p_{-\perp}\ ,\quad k_{3D}=p_{+\perp}\ ,\quad m_{1D}^2=m^2-p_{Dl}^2\ ,\quad m_{2D}^2=-(p_{Dl}-p_{-l})^2\ ,\quad m_{3D}^2=-(p_{Dl}+p_{+l})^2\ , \tag{22}$$

and the same for $I_X^{(m,0,z)}$ by changing the index to X.

On the other hand, for x and y, the numerator depends on $p_\perp$, over which we have to integrate. This integral is the simplest type of a so-called tensor integral, and it is clear that it can be split into two parts:

$$I_D^{(x,y)}=-\frac{1}{2\gamma^2\beta}(-p_{-\perp}I_D^2+p_{+\perp}I_D^3) \tag{23}$$

and the corresponding result for $I_X^{(x,y)}$. I_D^2 and I_D^3 are again standard Feynman integrals found in Appendix A:

$$I_D^{(2,3)}=I^{(2,3)}(k_{2D},k_{3D},m_{1D}^2,m_{2D}^2,m_{3D}^2) \tag{24}$$

and the corresponding result for $I_X^{(2,3)}$.

We finally get

$$\begin{aligned}\hat{M}=i\frac{2(Z\alpha)^2}{\beta}[&\not{w}^{(1)}(\not{p}_{Dl}+m)\not{w}^{(2)}I_D^S-\not{w}^{(1)}\not{p}_{-\perp}\not{w}^{(2)}I_D^2+\not{w}^{(1)}\not{p}_{+\perp}\not{w}^{(2)}I_D^3\\&+\not{w}^{(2)}(\not{p}_{Xl}+m)\not{w}^{(1)}I_X^S-\not{w}^{(2)}\not{p}_{-\perp}\not{w}^{(1)}I_X^2+\not{w}^{(2)}\not{p}_{+\perp}\not{w}^{(1)}I_X^3]\ .\end{aligned} \tag{25}$$

An alternative form for $\hat{M}$ can be found by using the properties of the Dirac spinors:

$$(\not{p}_+ +m)v(p_+)=0\ , \tag{26a}$$

$$\bar{u}(p_-)(\not{p}_- -m)=0\ . \tag{26b}$$

Rewriting them as

$$\not{p}_{+\perp}v(p_+)=-(\not{p}_{+l}+m)v(p_+)\ , \tag{27a}$$

$$\bar{u}(p_-)\not{p}_{-\perp}=-\bar{u}(p_-)(\not{p}_{-l}-m)\ , \tag{27b}$$

we get

$$\begin{aligned}\hat{M}=i\frac{2(Z\alpha)^2}{\beta}[&\not{w}^{(1)}(\not{p}_{Dl}+m)\not{w}^{(2)}I_D^S-(\not{p}_{-l}-m)\not{w}^{(1)}\not{w}^{(2)}I_D^2+\not{w}^{(1)}\not{w}^{(2)}(\not{p}_{+l}+m)I_D^3\\&+\not{w}^{(2)}(\not{p}_{Xl}+m)\not{w}^{(1)}I_X^S-(\not{p}_{-l}-m)\not{w}^{(2)}\not{w}^{(1)}I_X^2+\not{w}^{(2)}\not{w}^{(1)}(\not{p}_{+l}+m)I_X^3]\ .\end{aligned} \tag{28}$$

This form for $\hat{M}$ has been used to test the correctness of our calculations, as well as its numerical stability.

Let us now come back to the inclusion of the form factor $F(q^2)$. It is easy to see that this only changes the form of I_D to

$$I_D^{(m,i)}=\frac{1}{2\gamma^2\beta}\int d^2p_\perp\{m,p_i\}\frac{F((p_- -p)^2)F((p_+ +p)^2)}{(p_- -p)^2(p^2-m^2)(p_+ +p)^2}\bigg|_{p_l=p_{Dl}} \tag{29}$$

and similar for I_X, using p_{Xl} instead of p_{Dl}.

Now we can use the property of the dipole form factor

$$\frac{F(q^2)}{q^2}=\frac{\Lambda^2}{(\Lambda^2-q^2)q^2}=\frac{1}{q^2}+\frac{1}{\Lambda^2-q^2}\ , \tag{30}$$

which allows us to rewrite the integrals as the sum and difference of four integrals of the type, which we have already solved in terms of the elementary Feynman integrals. The scalar and tensor integrals corresponding to (21) and (24) are

$$\begin{aligned}I_D^{(S,2,3)}=&I^{(S,2,3)}(k_{2D},k_{3D},m_{1D}^2,m_{2D}^2,m_{3D}^2)-I^{(S,2,3)}(k_{2D},k_{3D},m_{1D}^2,m_{2D}^2+\Lambda^2,m_{3D}^2)\\&-I^{(S,2,3)}(k_{2D},k_{3D},m_{1D}^2,m_{2D}^2,m_{3D}^2+\Lambda^2)+I^{(S,2,3)}(k_{2D},k_{3D},m_{1D}^2,m_{2D}^2+\Lambda^2,m_{3D}^2+\Lambda^2)\end{aligned} \tag{31}$$

which we use in formulas (25) and (28) for $\hat{M}$.

The same can be done with the double dipole form factor (see also Appendix B)

$$\frac{F(q^2)}{q^2}=\frac{1}{q^2}+c_1\frac{1}{\Lambda_1^2-q^2}+c_2\frac{1}{\Lambda_2^2-q^2}\ , \tag{32}$$

giving a sum total of nine standard Feynman integrals.

$\hat{M}$ is now used in order to calculate the trace $\mathrm{Tr}[(\not{p}_-+m)\hat{M}(\not{p}_+-m)\hat{M}]$. For this tedious, but straightforward calculation, we have used a symbolic calculation program (FORM [10]).

Some care has been taken in evaluating these long expressions numerically, in order to avoid some of the large cancellations which normally occur in the scalar products. That these cancellation do occur can be shown, e.g., in m_{2D}^2, where they can be seen very easily:

$$\begin{aligned} m_{2D}^2&=-(p_{Dl}-p_{-l})^2\\ &=(p_D-p_{-z})^2-(\epsilon_D-\epsilon_-)^2\\ &=\frac{1}{4}\frac{1}{\gamma^2\beta^2}[(\epsilon_-+\epsilon_+)+\beta(p_{-z}+p_{+z})]^2\ , \end{aligned} \tag{33}$$

where we have used the fact that $1-\beta^2=\gamma^{-2}$. We see that for large values of γ, m_{2D}^2 becomes very small, which means that the cancellations in the first expressions are very large.

To avoid these cancellations in the scalar products, we did not use the longitudinal parts of the four-vectors directly, but transformed them into light-cone variables. The longitudinal vectors we have are $w^{(1)}$, $w^{(2)}$, p_{+l}, p_{-l}, p_{lD}, and p_{lX}, transverse vectors only $p_{+\perp}$, $p_{-\perp}$.

For the light-cone variables, we define a "+" and a "−" component of an arbitrary vector v:

$$v_{\text{“}+\text{”}}=v_0+v_z,\quad v_{\text{“}-\text{”}}=v_0-v_z. \tag{34}$$

The scalar product between longitudinal vectors is then

$$(v,w)=\tfrac{1}{2}(v_{\text{“}+\text{”}}w_{\text{“}-\text{”}}+v_{\text{“}-\text{”}}w_{\text{“}+\text{”}})\ , \tag{35a}$$

$$(v,v)=v_{\text{“}+\text{”}}v_{\text{“}-\text{”}}\ . \tag{35b}$$

Generally, one of the variables "+", "−" is small, the other large. For example, $w^{(1)}_{\text{“}+\text{”}}=1+\beta$ is large, and $w^{(1)}_{\text{“}-\text{”}}=1-\beta$ is very small, because β is close to one. We calculate it using

$$w^{(1)}_{\text{“}-\text{”}}=1-\beta=\frac{(1-\beta)(1+\beta)}{(1+\beta)}=\frac{1}{\gamma^2 w^{(1)}_{\text{“}+\text{”}}}\ . \tag{36}$$

The same can be done with the other vectors, e.g., if $p_{+z},p_{-z}>0$, we calculate $p_{+,\text{“}+\text{”}}$ and $p_{-,\text{“}+\text{”}}$ directly and the other as

$$p_{+,\text{“}-\text{”}}=\frac{\epsilon_+^2-p_{+z}^2}{\epsilon_++p_{+z}}=\frac{m^2+p_{+\perp}^2}{p_{+,\text{“}+\text{”}}}\ , \tag{37a}$$

$$p_{-,\text{“}-\text{”}}=\frac{\epsilon_-^2-p_{-z}^2}{\epsilon_-+p_{-z}}=\frac{m^2+p_{-\perp}^2}{p_{-,\text{“}+\text{”}}}\ . \tag{37b}$$

IV. PAIR PRODUCTION IN DOUBLE EQUIVALENT-PHOTON APPROXIMATION

The equivalent-photon approximation (EPA) or Weizsäcker-Williams method has been used in the past to calculate electromagnetic processes in heavy-ion collisions [4,5]. It consists of replacing the electromagnetic field of the fast moving ion by a spectrum of real photons. Then one folds the photon cross section with the number of equivalent photons $N(\omega)$ to get the cross section for the heavy-ion process. In the double equivalent-photon approximation (DEPA), one replaces the field of both ions by equivalent photons, then folds with both photon distributions. Normally, one uses the total equivalent photon number, the one integrated over all impact parameters [11,12]. Recently also the b-dependent DEPA has been investigated by Baur and Ferreira Filho [13,14] and also by Vidović *et al.* [15]. One of the problems of the DEPA is—because the virtual photons with $q^2\neq 0$ are all replaced by real photons—we have to introduce a cutoff in q^2, to avoid the logarithmic divergence, even though the main contribution comes from that part where q^2 is small. The cutoff can also be interpreted as a cutoff in the impact parameter (in the case of the EPA, where only one ion is replaced by the photon spectrum), or a cutoff in the distance between the ion and the place where the interaction with the electron or positron takes place. Also, contributions coming from scalar photons are neglected. There has been some discussion about the choice of the cutoff. On the one hand, the form factor of the ion decreases the number of photons with large q^2. On the other hand, the matrix element decreases, if the momentum of the internal electron line $|p|$ is greater than m_e. Therefore we are not allowed to replace this matrix element with the one for the photo process (see, e.g., the discussion in Sec. VI in [12]).

The DEPA gives us, on the one hand, an independent check for the correctness of our results and, on the other hand, a test of the applicability of the DEPA in this case, especially to see if the cutoff is given by the form factor.

For our calculation, we use the formula given by Baur and Ferreira Filho [13]. For $b=0$ their result is

$$dP(b=0)=\frac{d\omega_1}{\omega_1}\frac{d\omega_2}{\omega_2}\int d^2\rho N(\omega_1,\rho)N(\omega_2,\rho)\sigma_{\parallel}(\omega_1,\omega_2)\ , \tag{38}$$

where $\sigma_{\parallel}$ is the total cross section for pair production with the two photons with parallel polarization. $N(\omega,\rho)$ is the ρ-dependent equivalent-photon number. In the ultrarelativistic limit it is given by

$$N(\omega,\rho)=\frac{Z^2\alpha}{\pi^2}\frac{\phi(x,\rho)}{\rho^2} \tag{39}$$

with $x:=\omega\rho/\gamma c$ and

$$\phi(x,\rho)=\left|\int_0^\infty du\ u^2J_1(u)\frac{F(-(x^2+u^2)/\rho^2)}{x^2+u^2}\right|^2\ . \tag{40}$$

With a dipole form factor [Eq. (8)], we are splitting again $F(-(x^2+u^2)/\rho^2)/(x^2+u^2)$ into two parts:

$$\frac{\rho^2\Lambda^2}{\rho^2\Lambda^2+x^2+u^2}\frac{1}{x^2+u^2}=\frac{1}{x^2+u^2}-\frac{1}{\rho^2\Lambda^2+x^2+u^2}\ , \tag{41}$$

rewriting ϕ as

$$\phi(x,\rho)=\left|\int_0^\infty du\ u^2J_1(u)\left[\frac{1}{x^2+u^2}-\frac{1}{\rho^2\Lambda^2+x^2+u^2}\right]\right|^2 . \tag{42}$$

The integral

$$\int_0^\infty du\ u^2J_1(u)\frac{1}{z^2+u^2}=zK_1(z) \tag{43}$$

can be solved analytically, giving for ϕ the result for a point source, which is known. Therefore $\phi(x,\rho)$ is given by

$$\phi(x,\rho)=|xK_1(x)-\sqrt{\rho^2\Lambda^2+x^2}K_1(\sqrt{\rho^2\Lambda^2+x^2})|^2 \tag{44}$$

and using the definition of x, we find

$$N(\omega,\rho)=\frac{Z^2\alpha}{\pi^2}\left|\frac{\omega}{\gamma}K_1\left[\frac{\omega}{\gamma}\rho\right]-\left[\frac{\omega^2}{\gamma^2}+\Lambda^2\right]^{1/2}K_1\left[\left[\frac{\omega^2}{\gamma^2}+\Lambda^2\right]^{1/2}\rho\right]\right|^2 . \tag{45}$$

The cross section for real photons is [12]

$$\sigma_\parallel=\frac{4\pi\alpha^2}{s}\left[\left[1+\frac{4m^2}{s}-\frac{12m^4}{s^2}\right]L-\left[\frac{1}{s}+\frac{6m^2}{s^2}\right]\Delta t\right] \tag{46}$$

with

$$\begin{aligned} s&=4\omega_1\omega_2\ ,\\ \Delta t&=s\left[1-\frac{4m^2}{s}\right]^{1/2}\ ,\\ L&=2\ln\left[\frac{\sqrt{s}}{2m}+\left[\frac{s}{4m^2}-1\right]^{1/2}\right] . \end{aligned} \tag{47}$$

For the total probability we integrate over $d\omega_1$, $d\omega_2$, and $d^2\rho$ using a Monte Carlo (MC) integration routine (VEGAS [16,17]). The integration variables we use are $\ln\rho$, $\ln\omega_2$, and $\ln s$ and the boundaries of the integral have been increased until the result does not change. The accuracy of the MC integrals is always 1% or better.

V. THE TOTAL PROBABILITY P_{total}

The differential probability is now integrated over all six momentum variables. For this we used again the Monte Carlo integration routine [16,17]. The integration over one of the angles is trivial and an integration over five variables remains to be done, for which we used t_z, $t_\perp$, ϕ, η, and χ. The momenta of electron and positron expressed in these variables are

$$\begin{aligned} p_{+z}&=[\exp(t_z)-1]\cos\eta\ ,\\ p_{-z}&=[\exp(t_z)-1]\sin\eta\ ,\\ p_{+\perp}&=[\exp(t_\perp)-1]\cos\chi(1,0)\ ,\\ p_{-\perp}&=[\exp(t_\perp)-1]\sin\chi(\cos\phi,\sin\phi)\ . \end{aligned} \tag{48}$$

The integration boundaries in t_z and $t_\perp$ were incremented, until the MC integral converges. A good estimate for the boundaries is given by $\ln[\gamma\max(\Lambda,m_e)+1]$ for t_z and by $\ln[\max(\Lambda,m_e)+1]$ for $t_\perp$. The accuracy of the MC integrals was again 1% or less. Λ was chosen according to Appendix B as $\Lambda=83$ MeV for the dipole form factor and similarly for the double dipole form factor. In this section we will only discuss the probability divided by $(Z\alpha)^4$, as this is a common factor in our formula.

Figure 3 shows the dependence of the total probability on Λ for two different values of γ (100 and 3400). We see that there is a logarithmic dependence on Λ, so that the result seems to be divergent for a point charge. This divergence is, of course, no contradiction to the fact that the total cross section for a point charge

$$\sigma=\int 2\pi b\ dbP(b) \tag{49}$$

is finite.

Figure 4 shows $P_{\text{total}}/(Z\alpha)^4$ as a function of γ. We use the dipole form factor as well as the double dipole form factor. The difference between both is very small. This confirms our assumption that the detailed form of the form factor is not important, as only small q^2 contributes considerably to the total probability. Together with our calculation, we also plot the results of the EPA calculation for different values of the impact parameter b (formula 7.3.10 in [11], where we have neglected the term with $\bar{f}$). One sees that our calculation for $b=0$ only increases linearly with $\ln\gamma$, whereas the EPA result increases with $(\ln\gamma)^2$. Even for $b\approx\lambda\!\!\!^{-}_C$ the EPA result is larger than our result for $b=0$. As the probability should

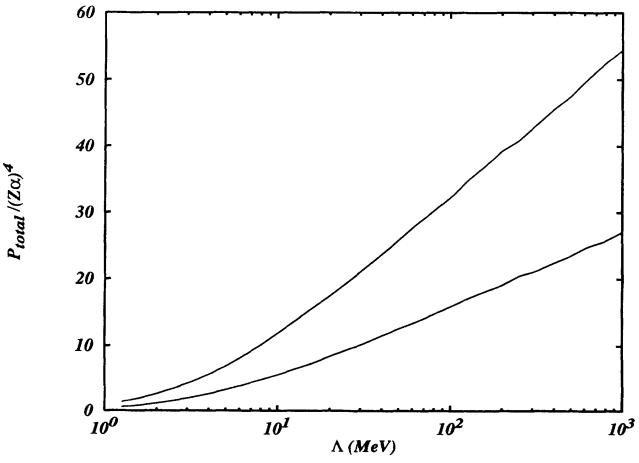

FIG. 3. $P_{\text{total}}/(Z\alpha)^4$ for $b=0$ as a function of Λ for $\gamma=100$ (lower curve) and 3400 (upper curve). The logarithmic increase shows that a form factor is needed, as the result for a point charge seems to diverge.

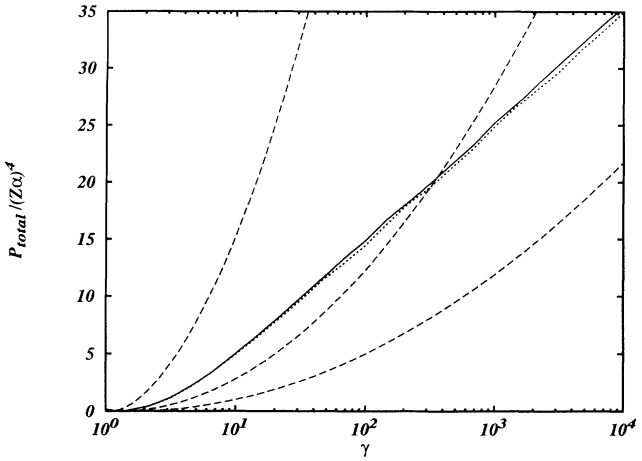

FIG. 4. $P_{\text{total}}/(Z\alpha)^4$ for $b=0$ as a function of γ for the creation of an electron-positron pair. The solid line is the calculation for a realistic dipole form factor, the dotted line for a realistic double dipole form factor (see Appendix B). The dashed lines are EPA results for impact parameters $b=0.5\lambda\!\!\!^{-}_C$, $b=1.0\lambda\!\!\!^{-}_C$, and $b=1.5\lambda\!\!\!^{-}_C$ (from left to right), respectively.

always increase with smaller impact parameter, we conclude that the EPA result cannot be used for small impact parameter and that the range, where it is not applicable, even increases slowly for larger values of γ. This result is, of course, well known, therefore formula 7.3.10 in [11] has always been used only for impact parameter $b > \lambda\!\!\!^{-}_C$.

We also note, that the total probabilities are not very large. Values smaller than 35 have to be multiplied by $(Z\alpha)^4 < 0.2$. Therefore the total probability is smaller than 7 for realistic parameters

Figure 5 shows again the total probability, but now together with those for μ and τ pairs. Their probabilities are much smaller due to the larger mass of the μ and the

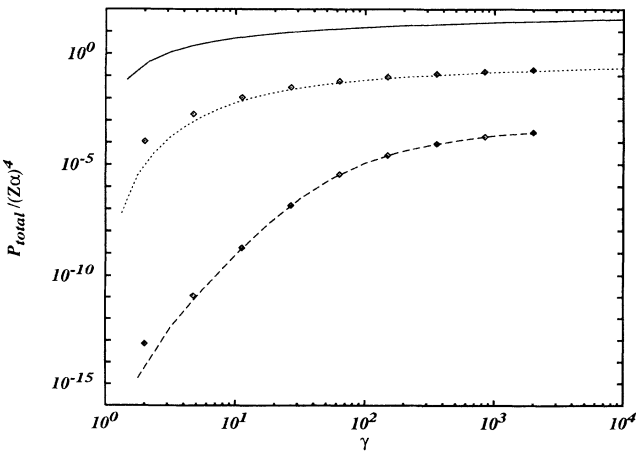

FIG. 5. $P_{\text{total}}/(Z\alpha)^4$ for $b=0$ as a function of γ for the creation of an electron (solid), μ (dotted), and τ pair (dashed). Results of the calculation with a dipole form factor. Also shown are the results of the DEPA calculation for μ and τ pairs (diamonds), also for a dipole form factor.

TABLE I. Predicted values of P_{total} for different accelerator parameters. AGS is the alternating-gradient synchrotron and SSC the superconducting supercollider.

	γ	Ion	P_{total}
AGS	2.35	Au	0.06
CERN SPS	10	Pb	0.63
RHIC	100	Au	1.6
LHC	3400	Pb	3.9
SSC	8000	Pb	4.4

τ. Also shown are the results of the DEPA calculation for the heavy ions. As their masses are much larger than Λ, the DEPA is in good agreement with the exact calculation. The deviation at small γ is due to the fact that the DEPA can only be used for relativistic collisions.

Finally, in Table I we give our predictions for the total probability for the electron-positron pair production for some heavy-ion accelerators.

We now compare the calculation with the DEPA result. Now each of the ions has its own form factor independent of the other, in order to study the influence of the individual form factor on the total probability.

In Fig. 6 we compare our calculation with the DEPA at relativistic heavy-ion collider (RHIC) energies ($\gamma=100$). We show $P_{\text{total}}/(Z\alpha)^4$ as a function of Λ_1 (the parameter controlling the width of one dipole form factor); Λ_2 for the other ion has been kept fixed. This comparison clearly shows that the DEPA massively overestimates the Born calculation, as soon as one and even more if both Λ's are larger than the electron mass. Therefore the reduction in q^2 due to the form factors does not suffice, the decrease of the matrix element of the process itself as soon as the internal momentum of the fermion gets larger than m_e is more important. But even then, this decrease alone does not suffice, as the total probability still depends on the form factor.

We see also that the probability becomes independent of Λ_1, if it is much larger than m_e and Λ_2. This corre-

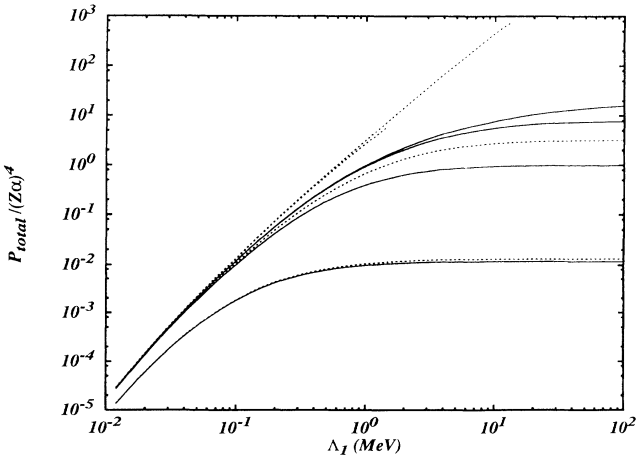

FIG. 6. A comparison of our calculation (solid) and the DEPA (dotted) for $\gamma=100$ as a function of Λ_1 of one ion. Λ_2 of the other ion has been kept fixed at $\Lambda_2=0.1$, 1, 10, and 100 MeV (from bottom to top).

sponds to the result that the production of a pair by a photon in the field of a nucleus is independent of the size of the nucleus, if the size is much smaller than the Compton wavelength.

VI. THE SINGLE-DIFFERENTIAL PROBABILITIES

Beside the total probability, we have also calculated some of the single-differential probabilities. For this, we have used the fact that with a MC integration single-differential distributions can be calculated very easily, sorting the individual integration points into bins. Therefore, one run of the program can be used to calculate several differential probabilities at once. A disadvantage of this method is that a large number of sample points is needed, if we want to get some accuracy, because the result spans several orders of magnitude. Again, as in the previous case, a common factor $(Z\alpha)^4$ has been extracted from P.

All calculations were done for CERN Super Proton Synchrotron (SPS), RHIC and large hadron collider (LHC) energies—that is for $\gamma=10$, 100, 3400—using both the simple dipole and the double dipole form factor. Generally, our results show some difference for the two form factors, but only a very small one, so that our results should represent the real situation well.

Figure 7 shows the dependence on the energy of the positron (as the result is symmetric with respect to electron and positron, this is the same for the electron). The probability has the characteristic peak at low energies and decreases for higher energies.

Figure 8 shows the angular distribution, where θ is the angle between the momentum p_+ and the beam axis (z axis). For large values of γ, the particles are produced mainly at very small angles.

We also study the distributions related to the total momentum $P=p_+ + p_-$. These are the invariant mass $M=\sqrt{P^2}$ and the rapidity

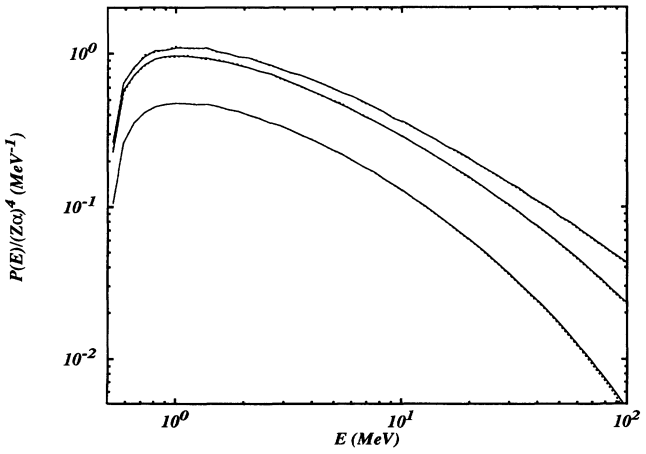

FIG. 7. $P(E)/(Z\alpha)^4$ as a function of the energy of the positron. Results for $\gamma=10$, 100, 3400 (from bottom to top) are shown, solid lines are the results using the realistic dipole form factor, dotted lines using the realistic double dipole form factor.

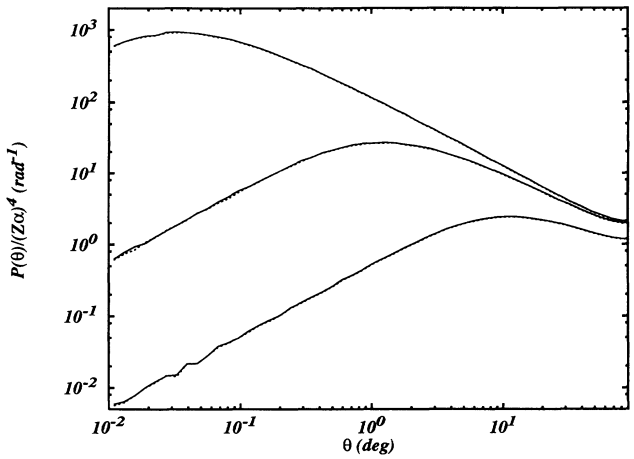

FIG. 8. $P(\theta)/(Z\alpha)^4$ as a function of the angle θ of p_+ with the z axis. γ and form factors as in Fig. 7.

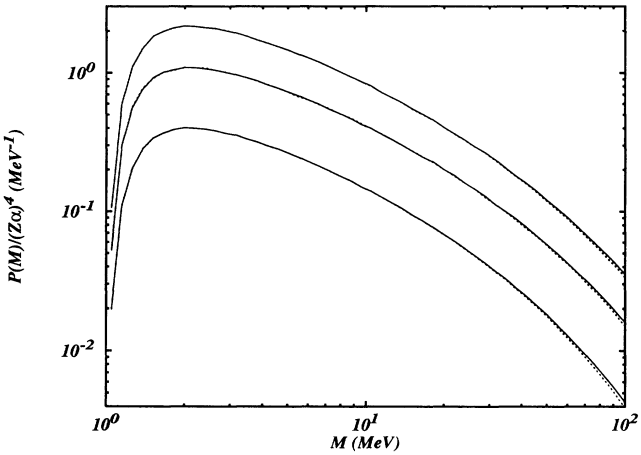

FIG. 9. $P(M)/(Z\alpha)^4$ as a function of the invariant mass M. γ and form factors as in Fig. 7.

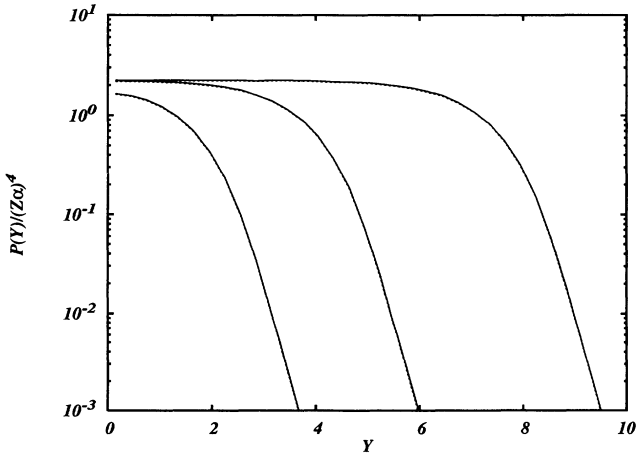

FIG. 10. $P(Y)/(Z\alpha)^4$ as a function of rapidity of the pair. γ and form factors as in Fig. 7.

$$Y=\frac{1}{2}\ln\left[\frac{P_0+P_z}{P_0-P_z}\right].$$

They are shown in Figs. 9 [$P(M)$] and 10 [$P(Y)$]. We show only $P(M)$ for relatively small values of M. A discussion of the behavior of $P(M)$ for large invariant mass can be found in the next section.

VII. A COMPARISON WITH DEPA FOR LARGE INVARIANT MASS

Finally we want to discuss the case where the invariant mass of the two leptons is large. It has been argued that in this case the DEPA approximation, which failed at low invariant mass, should again be applicable. This is based on the fact that in this case the only relevant momentum scale is the invariant mass, so that one may neglect effects coming from the electron mass.

Figure 11 shows a comparison of $P(M)$ between the DEPA and our calculation. Even though the difference between both is not that bad for large invariant mass, the DEPA is off by about a factor of 2.

The same can be seen in Fig. 12, where we compare $P(M,Y)$ for rapidity $Y=0$.

For the calculation of $P(M,Y=0)$ we have used the fact that for $Y=0$ (which means that $p_{+z}=-p_{-z}$) and with fixed M, p_{+z} and p_{-z} can be calculated as a function of the transverse momenta $p_{+\perp}$ and $p_{-\perp}$ together with their angle ϕ. The remaining three-dimensional integration was again done with the MC integration routine with an error of 1%. For the DEPA calculation, $Y=0$ and fixed M means that ω_1 and ω_2 are fixed at $M/2$, and only the integration over ρ has to be done. As σ is a function of M alone, we can use formula (46) again; see also [18]. We see again that the result of the DEPA is too large by a factor of 2.

This seems to be in contradiction with the arguments given above. In order to see where the discrepancy comes from, we calculated also $P(M,Y,\Omega)$. For the Born calculation we used again the sorting of P into bins. For the DEPA calculation, the differential cross section for the photon-photon process [8] has been used; see also [19].

We show $P(M,Y=0,\Omega)$ in Fig. 13 as a function of θ, the angle of p_+ with the beam axis. For large angles, the DEPA and our calculations agree quite well, but for small angles the DEPA calculation is too high. As one may object that this is an effect of the integration over the transverse momenta in the DEPA, which should smear out the angular distribution, we show in Fig. 14 $P(M,Y=0,\Omega_\Delta)$ as a function of θ_Δ, the angle of (p_+-p_-) with the beam axis. For the DEPA, in the form used by us, the two particles are produced with

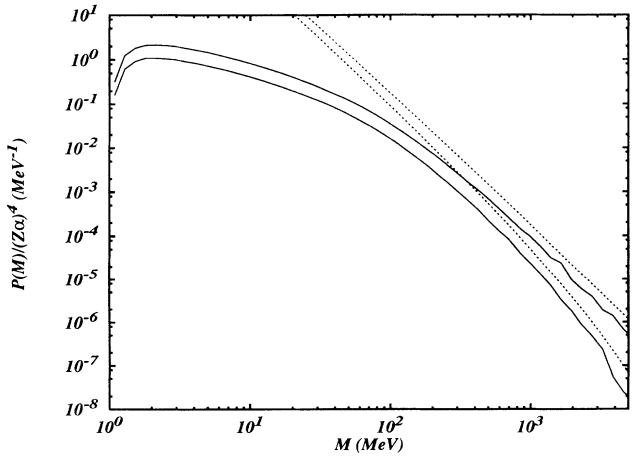

FIG. 11. $P(M)/(Z\alpha)^4$ is shown as a function of M for pairs with large invariant mass M. Comparison for $\gamma=100$ and 3400 of our calculation (solid line) with the DEPA (dotted line), using a realistic dipole form factor in both cases.

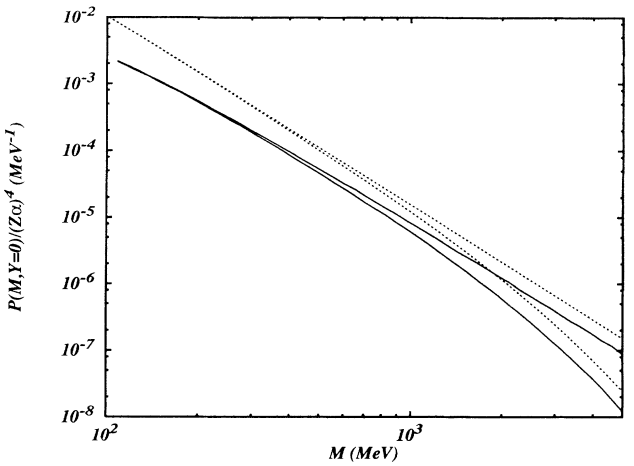

FIG. 12. $P(M,Y=0)/(Z\alpha)^4$ as a function of M. Comparison for $\gamma=100$ (lower curve) and 3400 (upper curve) of our calculation (solid line) with the DEPA (dotted line). Results for the realistic double dipole form factor are shown.

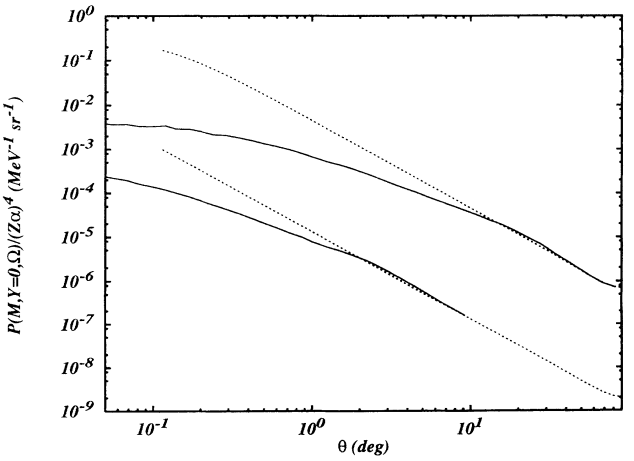

FIG. 13. $P(M,Y=0,\Omega)/(Z\alpha)^4$ as a function of the angle θ between p_+ and the z axis. Compared are the results of our calculation (solid line) and the DEPA (dotted line). $\gamma=3400$, $M=500$ MeV (upper curve), 3500 MeV (lower curve). Results for the realistic double dipole form factor are shown.

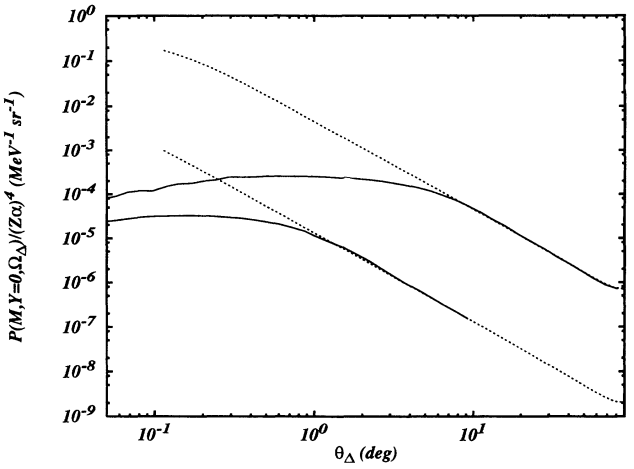

FIG. 14. Same as Fig. 13, but now $P(M,Y=0,\Omega_\Delta)/(Z\alpha)^4$ as a function of the angle θ_Δ between $(p_+ - p_-)$ and the z axis.

their momenta exactly opposite to each other, so the curve is identical with the previous one (see [18] for a better calculation, where the transverse momentum distribution has been included in the DEPA). But in our calculation, we should be able to unfold with this approximately the transverse momentum distribution coming from the virtual photons. Here again, we find good agreement at large angles, but the DEPA is too large at small ones.

The reason for this can be explained as follows: The total cross section for the pair production in lowest order by a photon in the electromagnetic field of a nucleus is given by the Bethe-Heitler formula [20]

$$\sigma=\frac{28}{9}\frac{Z^2\alpha^3}{m_e^2}\ln\frac{E_\gamma}{m_e} . \tag{50}$$

The logarithmic term in this formula is due to the pairs, which are produced at very small angles. This behavior is due to a so-called mass singularity in the matrix element, the fact that the propagator of the internal particle is very large, and even would become singular for $m_e\to 0$. But this behavior is connected to the fact that we are looking at a real photon with $q^2=0$. In the DEPA or EPA we neglect the dependence of the matrix element on the transverse momentum. But as q^2 is mainly given by $q_\perp^2$, this is only justified, as long as $q_\perp$ is smaller than m_e, whereas the form factor of the ions allows $q_\perp$ to be as high as 83 MeV. That is, we are not allowed to neglect m_e compared with M even for very large M, because setting $m_e=0$ would make our cross section divergent. There are always three momentum scales given by M, Λ, and m_e. The equivalent photon method has to be modified in the region of small angles. This explains why the calculations of $P(M)$ and $P(M,Y=0)$ are too large, as they are integrated over the whole θ range. But as this error only shows up in a logarithmic term, the deviation of the DEPA is not that large, compared, e.g., with P_{total}, where the DEPA overestimates the result by orders of magnitude.

ACKNOWLEDGMENTS

We would like to thank Jos Vermaseren, Mario Vidović, and Niels Baron for their help and advice during some stages of this calculation.

APPENDIX A: THE TWO-DIMENSIONAL FEYNMAN INTEGRALS

In this section, we calculate all the two-dimensional integrals needed for the matrix element. The only integral that must be solved in terms of analytic functions is the one with a two-term denominator; the others can then be reduced to this one.

1. The two-term denominator

This is the integral of the form

$$I(k_2,m_1^2,m_2^2):=\int d^2q \times\{[q^2+m_1^2][(q+k_2)^2+m_2^2]\}^{-1} . \tag{A1}$$

Introducing standard Feynman parameters, we find

$$I=\int_0^1 dx\int d^2q\{[q^2+m_1^2]x +[(q+k_2)^2+m_2^2](1-x)\}^{-2} . \tag{A2}$$

Rearranging the term in brackets, the integral is

$$\begin{aligned} I&=\int_0^1 dx\int d^2q\{[q+k_2(1-x)]^2+k_2^2x(1-x)+m_1^2x+m_2^2(1-x)\}^{-2} \\ &=\pi\int_0^1 dx\,[k_2^2x(1-x)+m_1^2x+m_2^2(1-x)]^{-1} . \end{aligned} \tag{A3}$$

The evaluation of the last integral is straightforward and we get

$$I(k_2,m_1^2,m_2^2)=\pi\ln\left[\frac{(k_2^2+m_1^2+m_2^2+s)^2}{4m_1^2m_2^2}\right]\Big/[(m_1^2-m_2^2)^2+k_2^2(k_2^2+2m_1^2+2m_2^2)]^{1/2} \tag{A4}$$

with

$$s:=[(k_2^2+m_2^2+m_1^2)^2-4m_1^2m_2^2]^{1/2} . \tag{A5}$$

Note that the final result only depends on the values of k_2^2, m_1^2, and m_2^2.

2. The three-term denominator

This is the integral

$$I^S(k_2,k_3,m_1^2,m_2^2,m_3^2):=\int d^2q\{[q^2+m_1^2][(q+k_2)^2+m_2^2][(q+k_3)^2+m_3^2]\}^{-1} . \tag{A6}$$

In principal, an analytic form can be found directly by doing the integration over the two auxiliary variables, using the trick described by t'Hooft and Veltman [21]. This calculation is rather tedious and it is easier to use a formula by van Neerven and Vermaseren [22] for the reduction of an $(N+1)$-term integral in N dimensions into $N+1$ N-term integrals.

Their formula (20) in our notation is

$$\begin{aligned} I^S(k_2,k_3,m_1^2,m_2^2,m_3^2)=&\{(r_2k_3-r_3k_2)^2+4[k_2^2k_3^2-(k_2k_3)^2]m_1^2\}^{-1} \\ &\times(\{2[k_2^2k_3^2-(k_2k_3)^2]-r_2k_3^2-r_3k_2^2+(r_2+r_3)k_2k_3\}I(k_3-k_2,m_2^2,m_3^2) \\ &+(r_2k_3^2-r_3k_2k_3)I(k_3,m_1^2,m_3^2)+(r_3k_2^2-r_2k_2k_3)I(k_2,m_1^2,m_2^2)) , \end{aligned} \tag{A7}$$

with

$$r_2=m_2^2+k_2^2-m_1^2 , \quad r_3=m_3^2+k_3^2-m_1^2 . \tag{A8}$$

Note again, that the final result only depends on m_1^2, m_2^2, m_3^2, k_2^2, k_3^2, and k_2k_3.

3. The tensor integral

The only tensor integral which appears in our calculation is the one with one momentum in the numerator. Generally, all tensor integrals can be reduced to the scalar integrals. Here we use the method which is described, for example, in t'Hooft and Veltman [21].

The standard form of the integral is

$$I^i(k_2,k_3,m_1^2,m_2^2,m_3^2)=\int d^2q q^i\{[q^2+m_1^2][(q+k_2)^2+m_2^2][(q+k_3)^2+m_3^2]\}^{-1} . \tag{A9}$$

As k_2 and k_3 are the only variables in the integral with a vector character, the integral can be split into

$$I^i=k_2^iI^2+k_3^iI^3 . \tag{A10}$$

To find expressions for I^2 and I^3, we multiply with k_2 and k_3 and solve for I^2 and I^3:

$$I^2=[k_2^2k_3^2-(k_2k_3)^2]^{-1}[k_3^2(k_2I)-k_2k_3(k_3I)] , \tag{A11a}$$

$$I^3=[k_2^2k_3^2-(k_2k_3)^2]^{-1}[-k_2k_3(k_2I)+k_2^2(k_3I)] . \tag{A11b}$$

Now with the help of

$$qk_2=\tfrac{1}{2}\{[(q+k_2)^2+m_2^2]-(q^2+m_1^2)-r_2\} \tag{A12}$$

and similarly for qk_3, we get

$$\begin{aligned} (k_2I)=&\int d^2q(k_2q)\{[q^2+m_1^2][(q+k_2)^2+m_2^2][(q+k_3)^2+m_3^2]\}^{-1} \\ =&\tfrac{1}{2}I(k_3,m_1^2,m_2^2)-\tfrac{1}{2}I(k_3-k_2,m_2^2,m_3^2)-\tfrac{1}{2}r_2I^S(k_2,k_3,m_1^2,m_2^2,m_3^2) \end{aligned} \tag{A13}$$

and similarly for k_3I. We find finally for I^2 and I^3

$$\begin{aligned} I^2=&\{2[k_2^2k_3^2-(k_2k_3)^2]\}^{-1}[(k_2k_3-k_3^2)I(k_3-k_2,m_2^2,m_3^2)+k_3^2I(k_3,m_1^2,m_3^2) \\ &-k_2k_3I(k_2,m_1^2,m_2^2)+(r_3k_2k_3-r_2k_3^2)I^S(k_2,k_3,m_1^2,m_2^2,m_3^2)] , \end{aligned} \tag{A14a}$$

$$\begin{aligned} I^3=&\{2[k_2^2k_3^2-(k_2k_3)^2]\}^{-1}[(k_2k_3-k_2^2)I(k_3-k_2,m_2^2,m_3^2)+k_2^2I(k_2,m_1^2,m_2^2) \\ &-k_2k_3I(k_3,m_1^2,m_3^2)+(r_2k_2k_3-r_3k_2^2)I^S(k_2,k_3,m_1^2,m_2^2,m_3^2)] . \end{aligned} \tag{A14b}$$

All integrals have been tested, using the symmetry of the formulas with respect to the exchange of the terms in the denominator and also using an identity between three integrals with different parameters, based on the property (2.2) of [21].

APPENDIX B: DISCUSSION OF THE FORM FACTORS

Normally a Gaussian form factor or that of a homogeneous charged sphere are used. They are given by (note that in our metric $q^2<0$):

$$F_{\text{Gauss}}(q^2)=\exp\left[-\frac{|q^2|}{2Q_0^2}\right], \tag{B1}$$

$$F_{\text{HCS}}(q^2)=\frac{3j_1(\sqrt{|q^2|}R_0)}{\sqrt{|q^2|}R_0}, \tag{B2}$$

with $Q_0=60$ MeV and $R_0=1.2$ fm $A^{1/3}\approx 7$ fm.

We are using two different form factors, which have the advantage that our matrix element can be expressed analytically with them. One is the dipole form factor

$$F_{\text{dipole}}(q^2)=\frac{\Lambda^2}{\Lambda^2-q^2}, \tag{B3}$$

which is the form factor of a Yukawa charge distribution

$$\rho(r)=\frac{\Lambda^2}{4\pi}\frac{\exp(-\Lambda r)}{r}. \tag{B4}$$

Λ has been determined so that the root mean square of the electric radius is equal to the experimental value

$$\sqrt{\langle r^2\rangle}=\left[\frac{6}{\Lambda^2}\right]^{1/2}=1\text{ fm }A^{1/3}, \tag{B5}$$

giving a Λ of about 83 MeV. This value has been used throughout the calculations, even though it varies slightly with A, for example, for Pb to Au.

A comparison of the different form factors can be found in Fig. 15. The disadvantage of the dipole form factor is that it decreases too slowly and overestimates the real value, if q is larger than about 50 MeV. To see if our result depends on the exact form of the form factor, we use a second one, which has a better behavior for large q. It is a sum of two dipole form factors:

$$F_{\text{double}}(q^2)=c_1\frac{\Lambda_1^2}{\Lambda_1^2-q^2}+c_2\frac{\Lambda_2^2}{\Lambda_2^2-q^2}. \tag{B6}$$

Therefore we call it a "double dipole form factor." With $F(0)=1$, we have $c_1+c_2=1$. The behavior of this form factor for large values of $|q|$ is

$$F(q^2)\sim\frac{\Lambda_1^2\Lambda_2^2-(c_1\Lambda_1^2+c_2\Lambda_2^2)q^2}{q^4}. \tag{B7}$$

For that the form factor vanishes faster than $1/q^2$, the coefficient in front of q^2 has to be zero, therefore Λ_2^2 has to be chosen as

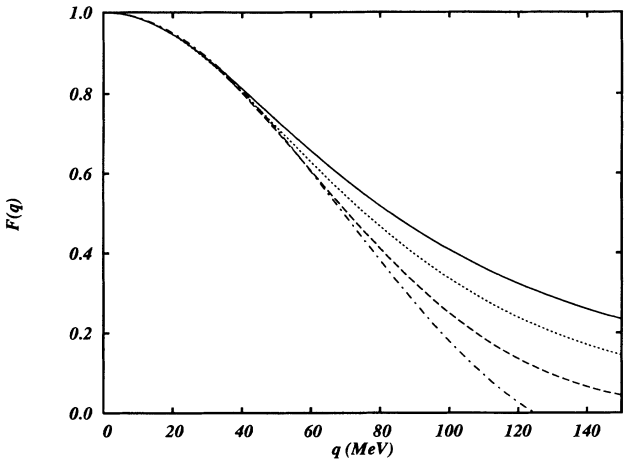

FIG. 15. A comparison of the different form factors. The dashed line is the gauss form factor and the dashed-dotted line the form factor of a homogeneously charged sphere. The solid line is the simple dipole form factor, the dotted line the double dipole form factor with parameter $c_1=10$.

$$\Lambda_2^2=-\frac{c_1}{c_2}\Lambda_1^2. \tag{B8}$$

As we do not want to have a singularity in the form factor, we have to choose $\Lambda_2^2>0$, that is, $c_1>1$. Finally, we want $\langle r^2\rangle$ to again be the same as the experimental one. As the density corresponding to this form factor is a sum of two Yukawa charge densities, $\langle r^2\rangle$ is

$$\langle r^2\rangle=6\left[\frac{c_1}{\Lambda_1^2}+\frac{c_2}{\Lambda_2^2}\right]. \tag{B9}$$

Therefore

$$\Lambda_1^2=\frac{6}{\langle r^2\rangle}\left[2-\frac{1}{c_1}\right], \tag{B10}$$

and c_1 is the only parameter, which can be varied. For $c_1=1$, we have the normal dipole form factor; for $c_1\to\infty$ it decreases faster than it. In Fig. 15 we have plotted $F_{\text{double}}(q)$ for $c_1=10$, a value that we have also used throughout the calculation, because the cancellations between the two dipole terms are not too large.

The reason why these form factors can be treated analytically is due to the fact that with the dipole form factor, we can write

$$\frac{F_{\text{dipole}}(q^2)}{q^2}=\frac{1}{q^2}\frac{\Lambda^2}{\Lambda^2-q^2}=\frac{1}{q^2}+\frac{1}{\Lambda^2-q^2}, \tag{B11}$$

having a term of the form $1/(q^2+m^2)$ again. Therefore our momentum integrals can be written as sums and differences of the standard Feynman integrals.

[1] G. Baur, Phys. Rev. A **42**, 5736 (1990).
[2] M. J. Rhoades-Brown and J. Weneser, Phys. Rev. A **44**, 330 (1991).
[3] C. Best, W. Greiner, and G. Soff, Phys. Rev. A **46**, 261 (1992).
[4] K. F. Weizsäcker, Z. Phys. **88**, 612 (1934).
[5] E. J. Williams, Phys. Rev. **45**, 729 (1934).
[6] J. Eichler, Phys. Rep. **193**, 165 (1990).
[7] L. D. Landau and E. M. Lifshitz, Phys. Z. Sowjet. **6**, 244 (1934).
[8] A. I. Achieser and W. B. Berestezki, *Quanten-Elektrodynamik* (B.G. Teubner Verlag, Leipzig, 1962).
[9] C. Bottcher and M. R. Strayer, Phys. Rev. D **39**, 1330 (1989).
[10] FORM is an algebraical calculation program by J. A. M. Vermaseren. The free version 1.0 can be found, e.g., at FTP.NIKHEF.NL
[11] C. A. Bertulani and G. Baur, Phys. Rep. **163**, 299 (1988).
[12] V. M. Budnev, I. F. Ginzburg, G. V. Meledin, and V. G. Serbo, Phys. Rep. **15**, 181 (1975).
[13] G. Baur and L. G. Ferreira Filho, Phys. Lett. B **254**, 30 (1991).
[14] G. Baur, Z. Phys. C **54**, 419 (1992).
[15] M. Vidović, M. Greiner, C. Best, and G. Soff, Phys. Rev. C **47**, 2308 (1993).
[16] G. P. Lepage, J. Comput. Phys. **27**, 192 (1978).
[17] G. P. Lepage, Cornell Laboratory for Nuclear Science Report No. CLNS-80/447, 1980 (unpublished).
[18] G. Baur and N. Baron, Nucl. Phys. **A561**, 629 (1993).
[19] N. Baron and G. Baur, Z. Phys. C **60**, 95 (1993).
[20] H. Bethe and W. Heitler, Proc. R. Soc. London **146**, 83 (1934).
[21] G. t'Hooft and M. Veltman, Nucl. Phys. **B153**, 265 (1979).
[22] W. L. van Neerven and J. A. M. Vermaseren, Phys. Lett. **B137**, 241 (1984).